Ionogel Electrolytes Supported by Zwitterionic Copolymers Featuring Lithium Ion-Mediated, Noncovalent Cross-links

*Karl W. Wieck and Matthew J. Panzer**

Department of Chemical and Biological Engineering, Tufts University

4 Colby Street, Medford, MA 02155, USA

*Corresponding author: matthew.panzer@tufts.edu

Abstract

A series of ionogel electrolytes, composed of an ionic liquid/lithium salt solution supported by a linear zwitterionic (ZI) copolymer scaffold containing solely noncovalent cross-links, was created in order to study the effects of varying the ZI fraction within the copolymer as well as the lithium ion concentration on gel mechanical properties and ion transport. The copolymer scaffold was synthesized via *in situ* UV photopolymerization of the ZI monomer 2-methacryloyloxyethyl phosphorylcholine (MPC) together with the non-ZI comonomer 2,2,2-trifluoroethyl methacrylate (TFEMA) in varying ratios, using a fixed fraction of 25 mol% total monomers. Ionic liquid

electrolyte (ILE) solutions of 0.1 M, 0.3 M, 0.5 M, or 1 M lithium bis(trifluoromethylsulfonyl)imide (LiTFSI) dissolved in the ionic liquid 1-butyl-1-methylpyrrolidinium bis(trifluoromethylsulfonyl)imide (BMP TFSI) were employed. For ionogels created using the 1 M LiTFSI ILE, varying the MPC content from 6.3 mol% to 17 mol% in the precursor solution resulted in a substantial increase in gel elastic modulus, from 20 kPa to 11 MPa. In contrast, room temperature ionic conductivity values for the same samples remained nearly constant, varying from 0.57-0.70 mS cm^{-1}. While the *in situ* photopolymerization approach remains highly versatile for ionogel formation, an alternative method is introduced here for the first time that can produce ionogels "on-demand" using a pre-made ZI copolymer/ionic liquid solution to which a Li^+ ILE is subsequently added.

Keywords: ionic liquids, gels, photopolymerization, phosphorylcholine, zwitterions, lithium

Introduction

Lithium-ion batteries (LIBs) are currently the energy storage system of choice for consumer electronics, as well as for the rapidly expanding application of electric vehicles. Current LIB technology allows for high energy density batteries that are relatively safe. However, there remains room for improvement in the safety aspects of the liquid electrolyte employed, which is composed of a lithium salt dissolved in flammable organic solvents.[1,2] While rare, fires and/or explosive incidents involving LIBs can lead to significant personal injury and property damage. An effective, nonflammable replacement for current organic solvent-based electrolytes is therefore

very desirable. Moreover, the future use of a lithium metal anode to further improve battery energy density will also require a highly stable, nonflammable electrolyte material.[3,4]

Ionic liquids (ILs) are nonvolatile liquids comprised of ambient temperature molten salts; that is, they consist solely of ionic species.[5,6] In recent years, ILs have emerged as a potential replacement for organic solvent-based electrolytes for battery electrolyte applications, where their nonvolatility, nonflammability, relatively high ionic conductivity, and large electrochemical stability windows are advantageous.[7,8] Typical ionic liquid electrolytes (ILEs) for batteries consist of an alkali metal salt dissolved in an IL.[7,9] Common ILEs employ bis(trifluoromethylsulfonyl)imide (TFSI) or bis(fluorosulfonyl)imide (FSI) anions, which contribute to low IL viscosity and the formation of a robust solid electrolyte interphase (SEI) layer on lithium metal anodes.[7] To further improve battery safety and performance, ionogel electrolytes have also been developed. Ionogels consist of an IL or ILE supported by a three-dimensional solid scaffold (*e.g.* a polymer network), which creates a stable, leakproof, mechanically robust composite electrolyte having a large liquid fraction, thus retaining a high room temperature ionic conductivity on the order of 1-10 mS cm^{-1}.[10,11]

When selecting a particular polymer scaffold for an ionogel battery electrolyte, there are many possible options. One particular class of recent interest is zwitterionic (ZI) polymers, which feature monomer units that contain both a positively charged and a negatively charged group, exhibiting a large dipole moment.[12,13] Previous research has shown the successful use of ZI polymers to form effective ionogel networks.[14–18] ZI side groups that are covalently bound to polymer chains can interact with one another to form noncovalent interchain cross-links due to Coulombic forces, which may yield a freestanding gel without the use of any covalent cross-linking agents.[19–21] The presence of certain ZI moieties can also maintain reasonable ionogel ionic

conductivity even while the elastic modulus is increased.[15,18,22,23] For example, it was previously demonstrated that ionogels supported by a fully-ZI copolymer of the two ZI comonomers 2-methacryloyloxyethyl phosphorylcholine (MPC) and sulfobetaine vinylimidazole (SBVI) could maintain a room temperature ionic conductivity comparable to that of the base ILE, even while possessing a high elastic modulus of 14.3 MPa.[18] More recently, the creation of ionogels with a sodium ion-based ILE having a polymer network that consisted of both MPC and SBVI diluted by a third non-ZI comonomer, 2,2,2-trifluoroethyl methacrylate (TFEMA), revealed that diluting the ZI copolymer composition by up to 60 mol% TFEMA still yielded freestanding gels with no significant drop in ionic conductivity.[15]

In this study, a systematic investigation of a binary, linear ZI copolymer scaffold-supported ionogel electrolyte system was conducted in order to examine the effects of the copolymer ZI fraction and the zwitterion:Li^+ molar ratio on the resulting gel electrical and mechanical properties, with the goal of yielding a better understanding of ionogel compositional design rules and the nature of the noncovalent cross-links formed within these nonvolatile, high-performance electrolytes. Ionogels were composed of a statistical copolymer network formed using one ZI and one non-ZI comonomer, MPC and TFEMA, respectively, which supported an ILE consisting of LiTFSI dissolved in 1-butyl-1-methylpyrrolidinium bis(trifluoromethylsulfonyl)imide (BMP TFSI). MPC was selected as the ZI comonomer due to the previously reported ability of its homopolymer to significantly boost the Li^+ transference number value when employed as the scaffold in an ionogel featuring a 1 M LiTFSI/BMP TFSI ILE.[24] Here, the phosphorylcholine groups of the MPC units were observed to coordinate effectively with lithium ions and form noncovalent cross-links that exhibited exceptional thermal stability (at least 45 min at 200 °C). For ionogels based on the 1M LiTFSI in BMP TFSI ILE, elastic modulus values were revealed to be

highly tunable, from approximately 20 kPa to 11 MPa, simply by varying the MPC (ZI) content from 6.3 to 17.4 mol%. Importantly, the room temperature ionic conductivity values of these materials remained relatively unchanged, varying between 0.57 and 0.70 mS cm^{-1}. These particular ionogels can therefore enable facile overall ion transport even while exhibiting a high elastic modulus of up to 11 MPa. In contrast to what was previously observed for poly(MPC) homopolymer scaffolds,[24] however, no significant boost in ionogel lithium transference number values was observed in this study, suggesting that the addition of TFEMA within the copolymer network may interrupt the formation of higher mobility pathways for Li^+ transport present along a fully-ZI scaffold. The insights gained here from examining the effects of ZI copolymer composition on ionogel properties shed additional light on the nature of the noncovalent, lithium ion-mediated ZI cross-links present in these systems, helping to further inform ZI polymer-based ionogel electrolyte design.

Experimental Section

Materials

The ionic liquid, 1-butyl-1-methylpyrrolidinium bis(trifluoromethylsulfonyl)imide (BMP TFSI, 99%, Iolitech Ionic Liquids Technologies GmbH), lithium bis(trifluoromethylsulfonyl)imide (LiTFSI, 99.95% trace metals basis, Sigma Aldrich), the photoinitiator, 2-hydroxy-2-methylpropiophenone (HOMPP, 97%, Sigma Aldrich), and the Celgard polyethylene/polypropylene separator material (MTI Corporation) were stored in a N_2-filled glove box (H_2O and O_2 < 0.1 ppm) until use. The ZI monomer, 2-methacryloyloxyethyl phosphorylcholine (MPC, 97%, Sigma Aldrich) and the comonomer 2,2,2-trifluoroethyl

methacrylate (TFEMA, Scientific Polymer Products, Inc.) were stored in a refrigerator until use. Polyethylene glycol diacrylate (PEGDA, Mn = 575 g mol^{-1}, Sigma Aldrich) was stored under ambient conditions and protected from light. Lithium metal foil (99.9%, Alfa Aesar) and stainless steel CR2032 coin cell parts (SS304 grade, MTI Corporation) were stored in an Ar-filled glove box (H_2O and O_2 < 0.5 ppm) until use. All materials were used as received.

Ionogel Preparation

ILE solutions of four concentrations of LiTFSI in BMP TFSI (0.1 M, 0.3 M, 0.5 M, and 1 M) were produced in a N_2-filled glove box by dissolving LiTFSI in BMP TFSI and stirring at 50 °C until transparent solutions were formed. These four solutions correspond to LiTFSI:BMP TFSI molar ratios of approximately 1:33, 1:11, 1:6.6, and 1:3.3, respectively. Ionogel precursor solutions were produced in a N_2-filled glove box by adding MPC and TFEMA monomers to the appropriate ILE solution and stirring at ambient temperature for 2-4 h, depending on monomer composition, until a homogeneous, transparent solution was formed. A fixed ratio of 75 mol% ILE solution to 25 mol% total comonomers was maintained for all samples in this work. After a visibly homogeneous ionogel precursor solution had been formed, the photoinitiator, HOMPP, was added (2 wt% of total comonomers basis) and stirred for one min, and then the precursor solution was used to fill the relevant mold or separator (see below) or left in the mixing vial for qualitative inspection. The precursor solution was then exposed to UV irradiation (365 nm) using a handheld lamp (Spectronic Corp., 8W) for 10 min, and the resulting ionogel was allowed to sit overnight inside the N_2-filled glove box before further characterization.

To prepare ionogel samples for room temperature ionic conductivity measurements, the precursor solution was transferred into cylindrical wells (volume ≈ 125 μL) in a custom

polytetrafluoroethylene (PTFE) apparatus with gold-coated electrodes prior to UV irradiation. To prepare ionogel samples for dynamic mechanical analysis (DMA) characterization or temperature-dependent ionic conductivity measurement, a mold was assembled from a PTFE washer between two glass slides, held together by binder clips. A slot was cut into the PTFE washer to allow the mold to be filled by a syringe needle. Polyethylene sheets were placed between the glass and PTFE, to prevent the ionogel from adhering to the glass. For DMA characterization, the PTFE washer had an inner diameter of 6.35 mm and a height of 3.15 mm; for temperature-dependent ionic conductivity measurement, the PTFE washer inner diameter was 5.12 mm and the height was 1.12 mm. For DMA characterization, the resulting ionogel was removed from the mold; for temperature-dependent ionic conductivity measurements, the glass and polyethylene layers were removed, but the PTFE washer/ionogel assembly was left intact for introduction into a coin cell (see below). To prepare ionogel samples for lithium transference number measurement, the precursor solution was soaked into a Celgard porous separator disc (17 mm diameter) under vacuum for 20 min, prior to UV irradiation.

Mechanical Measurements

Ionogel elastic modulus values were determined via compression testing using a dynamic mechanical analyzer (DMA) (RSA3, TA Instruments) under ambient conditions. A parallel-plate geometry was used in free extension mode, with an applied strain rate of 0.0315 mm s^{-1}. The elastic modulus was calculated as the slope of the linear region of the stress-strain data, approximately between 5% and 10% strain. Replicate samples typically yielded modulus values of <10% variation between them.

Electrochemical Measurements

Ionogel impedance was measured via electrochemical impedance spectroscopy (EIS) using a VersaSTAT 3 potentiostat with built-in frequency response analyzer (Princeton Applied Research). Room temperature ionic conductivity measurements were performed inside a N_2-filled glove box using a custom PTFE well apparatus, using a frequency range of 1 Hz to 100 kHz with a sinusoidal voltage amplitude of 10 mV.

Stainless steel|ionogel|stainless steel coin cells for temperature-dependent ionic conductivity measurements were assembled inside an Ar-filled glove box (H_2O and $O_2 < 0.5$ ppm). The ionogel sample/PTFE washer assembly was placed between two stainless steel discs (15.5 mm diameter, 0.5 mm thickness), with ~10 μL of ILE solution placed on each gel/stainless steel interface. These components were placed inside a CR 2032 coin cell case with a stainless steel wave spring, and crimped using an electric coin cell crimper (MSK-160E, MTI Corporation).

For temperature-dependent ionic conductivity determination, coin cells were placed on a temperature-controlled microscopy stage with resistive heating and liquid nitrogen cooling (LTS 420, Linkam Scientific Instruments), and EIS was performed using the VersaSTAT potentiostat. EIS spectra were recorded between 20 °C and 100 °C, with an isothermal hold of 15 min at each temperature to allow for thermal equilibration within the coin cell.

Symmetric lithium|ionogel|lithium coin cells for lithium transference number measurements were assembled inside an Ar-filled glove box (H_2O and $O_2 < 0.5$ ppm). Electrodes were obtained by punching out lithium metal foil discs (~11.1 mm diameter) and rolling these out using a glass vial onto stainless steel discs (15.5 mm diameter, 0.5 mm thickness) to cover the steel and to expose a shiny lithium surface. A Celgard separator disc containing the ionogel within its pores was placed between the two lithium electrodes, adding ~50 μL of ILE on each gel-lithium

metal interface. These components were placed inside a CR 2032 coin cell case and crimped as described above.

Lithium|ionogel|lithium coin cells were preconditioned using a 2 h galvanostatic charge step at 0.01 mA cm^{-2}, followed by a 2 h potentiostatic hold, followed by a 2 h galvanostatic discharge at -0.01 mA cm^{-2}, and finally a 12 h open circuit rest period. For lithium transference number (t_{Li^+}) value determination, the VersaSTAT potentiostat was used to conduct DC chronoamperometry polarization measurements at an applied potential (ΔV) of 10 mV until the resulting current reached a plateau (2-3 h depending on the sample); EIS spectra were collected before and after each polarization. The t_{Li^+} values were determined using the method developed by Bruce and co-workers,[25] via equation (1):

$$t_{Li^+} = \frac{I_{ss}(\Delta V - I_0 R_0)}{I_0(\Delta V - I_{ss} R_{ss})} \quad (1)$$

where I_0 and I_{ss} are the initial and steady state currents, respectively, and R_0 and R_{ss} are the initial and steady state interfacial resistance values measured via EIS before and after the DC polarization, respectively. Sample data used to determine steady state polarization currents and interfacial resistance values are shown in Figure S1 in the Supporting Information.

Results and Discussion

A series of ionogels was fabricated, wherein the ILE consisted of LiTFSI salt dissolved in BMP TFSI, and for which the supportive solid network was synthesized by *in situ* copolymerization of MPC and TFEMA monomers. Figure 1 shows the chemical structures of the main ionogel components. The ZI monomer, MPC, was selected because it has been previously shown to boost lithium ion transport in similar ionogels, and is commercially available.[24] TFEMA was selected as a non-ZI comonomer because it has previously been shown to be a miscible comonomer in ZI ionogel systems[15,26] and its inclusion in polymer electrolytes imparts a wide electrochemical stability window owing to its fluorination.[27,28] LiTFSI in BMP TFSI was selected as the ILE in this work because at a 1 M concentration, it is a commonly used ILE in ionogels for energy storage applications.[18,24,29,30] In addition to 1 M, this work also examined ionogels featuring ILEs of 0.5 M, 0.3 M, and 0.1 M LiTFSI in BMP TFSI, to study the effects of decreasing the concentration of lithium cations, which were expected to play a critical role in forming noncovalent cross-links within these systems.

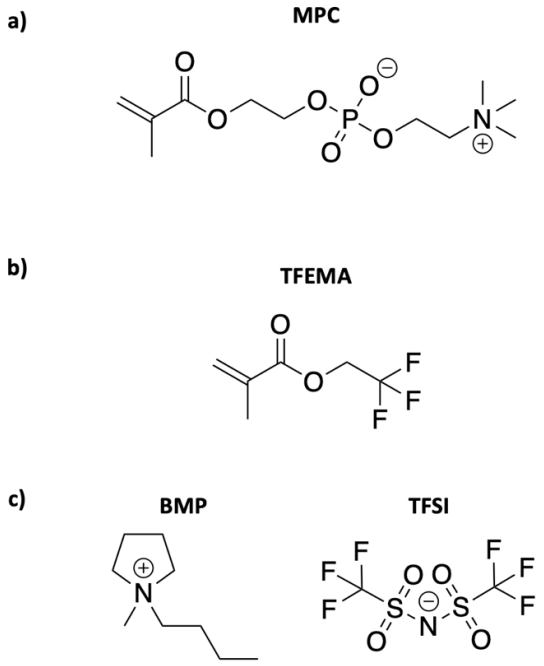

Figure 1. Molecular structures of: (a) ZI monomer MPC, (b) non-ZI comonomer TFEMA, and (c) the ionic liquid BMP TFSI.

Recent studies of ionogels supported by ZI copolymers have suggested that lithium-mediated, non-covalent cross-links form between at least two MPC units, creating robust polymer networks from linear ZI copolymer chains.[18,24] Figure 2 shows a schematic illustration of the non-covalent cross-linking expected in the present ionogel system, wherein lithium cations (shown as red circles) mediate interactions between phosphorylcholine side groups (of MPC monomers) on adjacent polymer chains to form cross-links between them via Coulombic forces. Experimental evidence from this study has revealed that both MPC monomers and Li^+ ions are necessary in order for non-covalent cross-linking to occur and to create a freestanding ionogel. As a control experiment, when MPC and TFEMA were copolymerized within neat BMP TFSI (without any LiTFSI present), no freestanding gels were produced. Similarly, when TFEMA was polymerized by itself in the ILE of 1 M LiTFSI in BMP TFSI, no freestanding gel was produced. Therefore, in

order for a cross-link to form, it is hypothesized that (at least) two MPC groups must simultaneously coordinate with a common lithium cation. Freestanding ionogels are formed when a sufficient density of cross-links exists to prevent the ILE-rich composite from flowing.

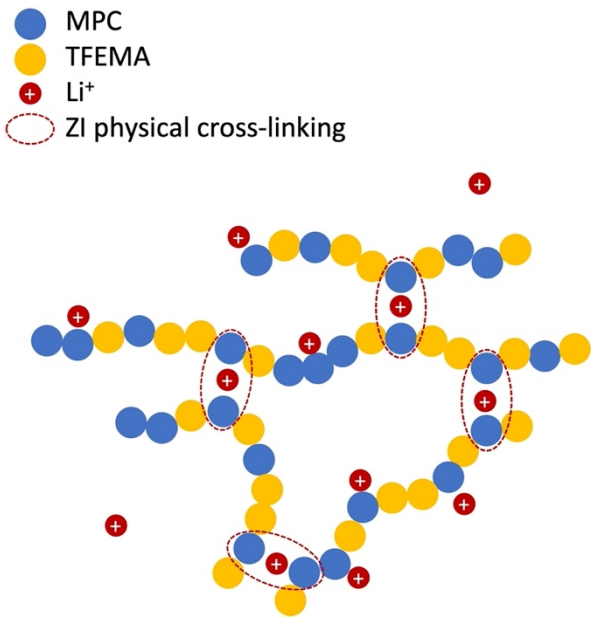

Figure 2. Illustration of the proposed lithium ion-mediated, noncovalent cross-linking mechanism responsible for the formation of the ionogels created in this study.

Figure 3a is a phase diagram illustrating the compositional range of MPC and lithium contents explored in this work, which displays the gelation status of the resulting sample fabricated at each point. Complete conversion of the co-monomers is assumed, since photopolymerization rates and product yields in IL systems are generally understood to be exceptionally efficient.[31] For certain compositions with a low MPC:Li^+ molar ratio and low MPC content, indicated by the points shown in yellow in Fig. 3a, the resulting product after UV polymerization was a viscous polymer solution, indicating that there were an insufficient number of noncovalent cross-links formed to create a freestanding gel. The majority of compositions examined in this work, however, indicated by points shown in orange, produced visibly transparent, freestanding ionogels upon

polymerization. Figure 3b shows a photograph of such an ionogel inside an inverted glass vial. For certain compositions with relatively high MPC:Li^+ molar ratios, polymerization of the transparent precursor solutions yielded white-colored, semi-opaque gels, which likely indicates poor solubility/phase separation of MPC-rich polymer regions; these are shown in Fig. 3a as blue data points. Figure 3c displays a sample of this gel type. All of the points shown on the phase diagram fall onto one of four solid lines indicated, which correspond to a fixed Li^+ concentration in the ILE: 0.1 M, 0.3 M, 0.5 M, or 1 M. The slope of each line is the Li^+ concentration within the sample in units of mol% (*i.e.* 2.2, 6.3, 9.8, or 17 mol% Li^+, respectively). The shaded triangular region highlights seven ionogel compositions labeled with letters that were selected for further characterization. The 1 M formulations within this region (points A, B, C, and D) may be considered most relevant for potential battery electrolyte applications, as this concentration of salt typically maximizes ionic conductivity in nonaqueous systems.[32] Points D, F, and G all possess a MPC:Li^+ molar ratio of 1, while points A, E, and G each possess a fixed MPC content of 6.3 mol% (1:3 MPC:TFEMA molar ratio), with varying Li^+ concentration in the ILE. The data shown in Fig. 3a reveal that lithium ions play a key role in solvating MPC repeat units within the ionogels, since copolymer scaffold compatibility with the ILE (*i.e.* formation of transparent gels) improves for larger MPC contents with increasing Li^+ concentration. The same is true for MPC monomer in the precursor solutions; we observed significantly lower solubility of MPC in the neat BMP TFSI ionic liquid than in the ILE solutions that contain LiTFSI.

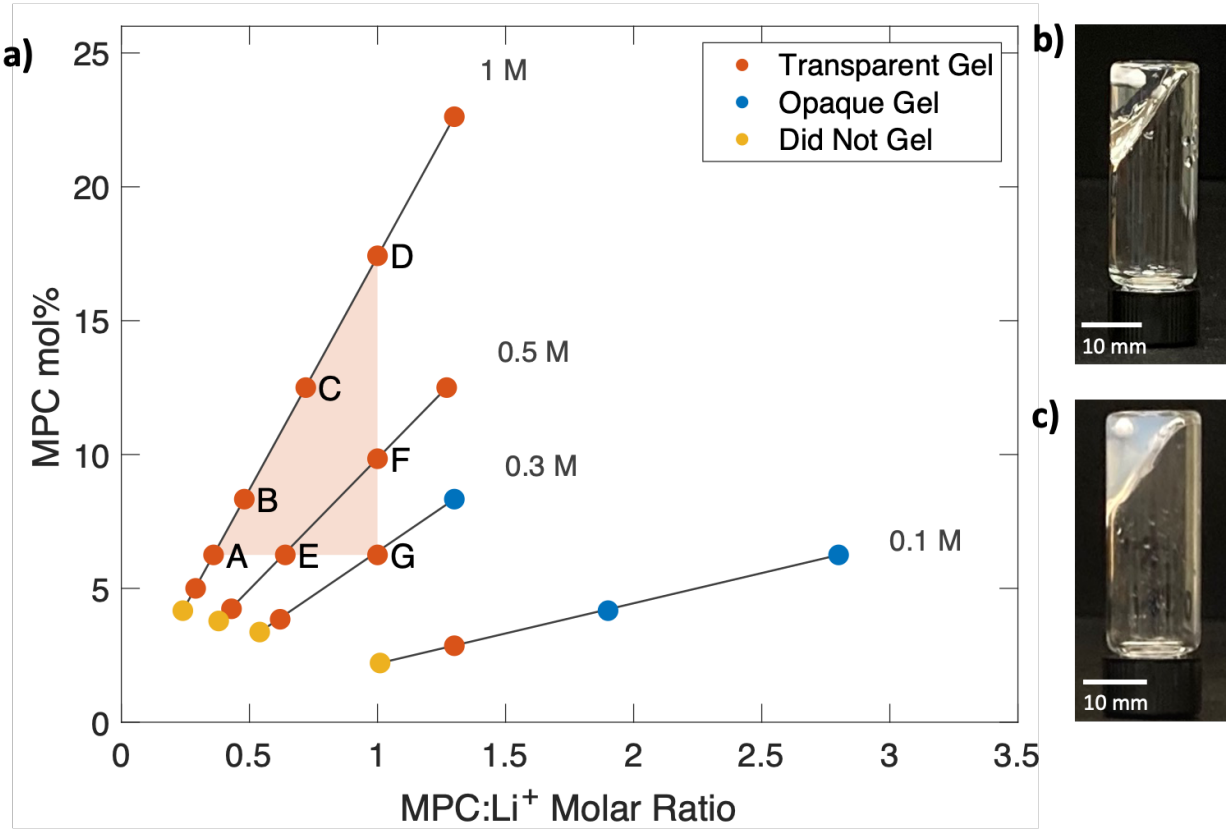

Figure 3. (a) Phase diagram illustrating the compositional design space of poly(MPC-co-TFEMA) copolymer-supported ionogels examined in this work. Black lines connect samples with constant LiTFSI concentration in the ILE. Orange points indicate compositions that yielded transparent freestanding gels, blue points indicate compositions that yielded opaque freestanding gels, and yellow points indicate compositions that did not produce freestanding gels. Compositions labeled with letters A-G in the shaded triangular region were selected for further characterization. **(b)** Photograph of a typical "transparent gel" sample. **(c)** Photograph of a typical "opaque gel" sample. Both samples shown in panels (b) and (c) were prepared by *in situ* UV copolymerization of a precursor solution while the glass vial was tilted at an angle (approximately 60° from vertical); the white object visible inside each ionogel is a stir bar that was left in place during the copolymerization step. The glass vials are inverted in both images, highlighting the nonflowing nature of the ionogels.

For each of the ILE Li^+ concentrations employed, the minimum amount of MPC required to create a freestanding gel was determined (see Fig. 3a, orange points directly adjacent to yellow

points on a given ILE molarity line). Figure 4 shows that the minimum MPC:Li^+ molar ratio required to form a freestanding gel depends approximately inversely on the lithium ion concentration in the ILE. The maximum MPC:Li^+ ratio observed not to form a freestanding gel at each ILE concentration (yellow points) follows a similar trend (see Figure S2). Thus, for a given lithium ion concentration, a certain minimum MPC:Li^+ ratio is necessary to create a sufficient density of Li^+-mediated ZI cross-links and yield a freestanding gel.

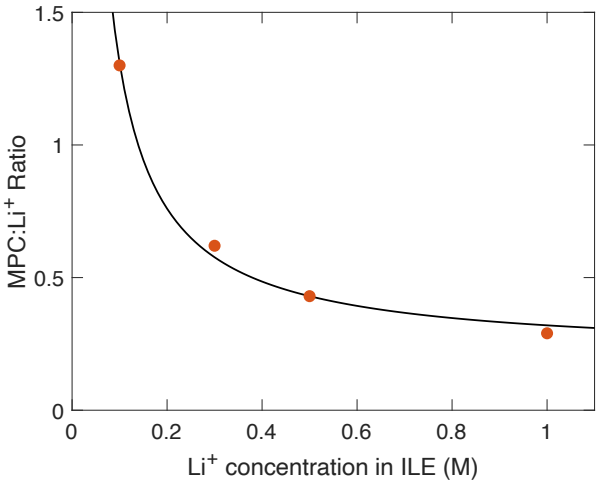

Figure 4. Minimum MPC:Li^+ molar ratio necessary to yield a freestanding ionogel determined for different ILE concentrations. The black curve is a nonlinear least-squares regression of the form $y = \frac{a}{x} + b$, shown to guide the eye.

A possible physical explanation for the small increase in the minimum MPC concentration needed to form freestanding gels at higher Li^+ concentrations (Fig. 3a) derives from recognizing that not all of the ZI MPC units are involved in cross-linking, as illustrated in Fig. 2. Some fraction of the MPC monomer is expected to coordinate with lithium ions within the well-mixed precursor solution, and among these assemblies, it is hypothesized that both singly-coordinated MPC-Li^+ complexes and doubly-coordinated MPC-Li^+-MPC complexes are formed. Only the latter are believed to subsequently become noncovalent cross-links within the ionogel scaffold (see Fig. 2)

upon polymerization of the precursor solution. In the presence of a greater background ILE Li^+ concentration, a higher fraction of singly-coordinated MPC-Li^+ complexes is expected to form; thus, these formulations would require a greater concentration of MPC monomer to achieve a sufficient density of cross-links for gelation to occur.

For selected ionogel samples (points A-G in Fig. 3a), the elastic modulus was measured in order to assess the extent of noncovalent cross-linking for various gel formulations. Figure 5a displays the elastic modulus of these ionogels plotted as a function of the MPC:Li^+ ratio and MPC mol% in the precursor solution, while Figure 5b displays the same values grouped by Li^+ concentration in the ILE. All values are also listed in Table S1, and representative stress vs. strain curves are shown in Figure S3. Clearly, the stiffness of these noncovalently cross-linked ionogels is highly tunable, between approximately 20 kPa and 11 MPa. The stiffest ionogels were observed to be brittle and did not exhibit self-healing properties when cut, suggesting that they are supported by cross-links that are highly robust and non-dynamic. Modulus values were found to increase significantly with increasing MPC mol% in the ionogel at a fixed MPC:Li^+ molar ratio of 1:1 (*i.e.* samples G vs. F vs. D), and to also increase along with a greater MPC:Li^+ ratio at a fixed MPC content of 6.3 mol% (*i.e.* samples A vs. E vs. G). The largest relative gain in gel stiffness was obtained upon increasing the MPC content at a fixed ILE concentration of 1 M (*i.e.* samples A vs. B vs. C vs. D). Notably, the highest modulus value achieved among gels A-G (11 MPa, sample D) was obtained for the largest MPC content (17.4 mol% MPC), which was enabled by a high ILE Li^+ concentration (1 M) that allowed this amount of ZI monomer to be dissolved in the precursor solution. Collectively, these findings support the hypothesis that a greater density of lithium ion-mediated noncovalent cross-links can be realized via polymerization of a precursor solution that contains a larger number of MPC-Li^+-MPC complexes. An upper limit in ionogel stiffness is

expected, however, as the solubility limit of LiTFSI in the ILE (and consequently, of MPC in the precursor solution) is approached.

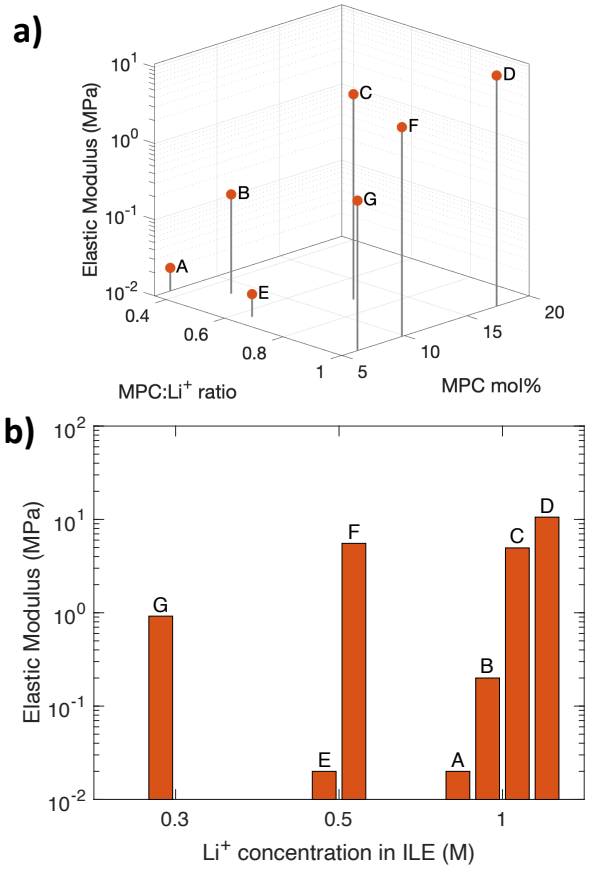

Figure 5. (a) Ionogel elastic modulus values plotted as a function of the MPC:Li^+ molar ratio and the MPC content (mol%) in the precursor solution. **(b)** Ionogel elastic modulus values displayed as a function of Li^+ concentration (molarity) in the ILE.

To probe the thermal stability of the noncovalent MPC-Li^+-MPC cross-links, a cylindrical ionogel of the composition referred to as "D" (consisting of 17.4 mol% MPC and 7.6 mol% TFEMA, polymerized in the 1 M ILE) was heated on a temperature-controlled microscopy stage to 200°C and held for 45 min at this temperature under an atmosphere of flowing nitrogen gas.

While the opacity of the sample increased and a small amount of ILE was observed to leach out of the bottom of the ionogel (approximately 20% of the initial mass) during heating, the original cylindrical shape of the gel was unchanged. After cooling the gel back down to room temperature, during which it did not re-swell with the small amount of leached ILE, its elastic modulus was remeasured via compressive stress-strain testing. Remarkably, the elastic modulus of the sample remained at approximately the same high value (8.6 MPa before the heat treatment, and 9.4 MPa afterwards; see Figure S4), demonstrating the outstanding thermal stability of these noncovalent MPC-Li^+-MPC cross-links. The onset of ionogel thermal degradation was observed to occur at approximately 300 °C, according to thermogravimetric analysis (Figure S5).

Room temperature ionic conductivity values of ionogel samples A-G were measured via EIS and are shown in Figure 6 (and tabulated in Table S1). Importantly, the ionic conductivity values of all samples lie between 0.57 mS cm^{-1} and 1.26 mS cm^{-1}, which represents a much smaller variation compared to that of their elastic modulus values. The most significant factor determining ionogel ionic conductivity is the Li^+ concentration in the ILE (grey bars topped with asterisks in Fig. 6). This is due to the increase in ILE viscosity at higher Li^+ concentrations, which results in lower ion mobilities and total ionic conductivity.[33,34] For the 1 M Li^+ ILE ionogel samples (A-D), it can be seen that increasing the ZI MPC fraction in the scaffold (D > C > B > A; see Fig. 3a) results in a slight upward trend in ionic conductivity. This is consistent with our previous finding that a ZI poly(MPC) homopolymer scaffold enabled a room temperature ionogel total ionic conductivity essentially equal to that of the 1 M ILE.[24] From this study, however, it is apparent that dilution of the ZI MPC units with a non-ZI co-monomer (TFEMA) in the copolymer scaffold leads to a reduction in the overall ionic conductivity.

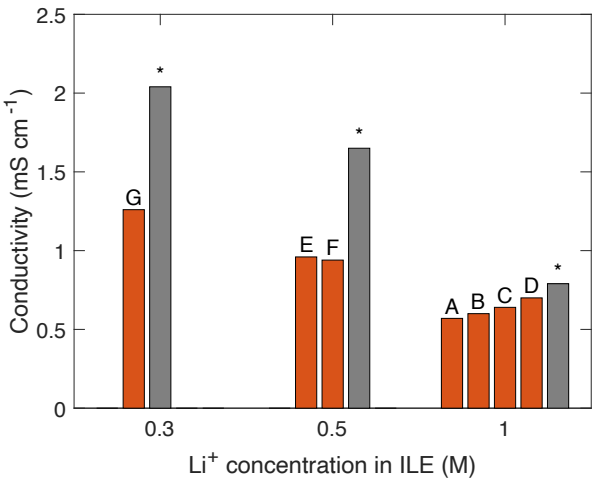

Figure 6. Ionogel ionic conductivity values (measured at room temperature) grouped by lithium ion concentration in the ILE. Grey bars topped with asterisks correspond to ionic conductivity values of the ILEs.

Figure 7 displays the temperature dependence of ionic conductivity for ionogel compositions "A" and "D" measured between 20 °C and 100 °C. While both of these gels are based on the same 1 M LiTFSI concentration in the ILE, ionogel "D" contains a nearly threefold larger ZI MPC content (17.4 mol% vs. 6.3 mol%). The temperature dependence of the ionic conductivity data was fit using the Arrhenius form given in equation (2):

$$\sigma = \sigma_0 e^{\left(\frac{-E_a}{RT}\right)} \tag{2}$$

where σ is the ionic conductivity, σ_0 is a prefactor constant, T is the absolute temperature, R is the universal gas constant, and E_a is the apparent activation energy of ionic conductivity. The value of E_a for an ionogel compared to that of its base ILE can provide important information about barriers to hopping-like transport within these ion-dense, liquid-rich electrolytes. While the apparent activation energy value obtained for gel "A" (29.4 kJ mol^{-1}) was similar to that of the 1

M ILE (29.2 kJ mol^{-1}),[24] the value for gel "D" with the MPC-rich scaffold was found to be somewhat lower (27.6 kJ mol^{-1}). This is in agreement with our previous study that revealed a clear reduction in E_a for a poly(MPC) homopolymer scaffold in the same ILE.[24] It is hypothesized that this behavior may be due to an ability of the ZI phosphorylcholine groups to dissociate some of the $Li^+(TFSI^-)_n$ clusters present within the ILE, thereby improving overall ion transport. To clarify any potential effect that the TFEMA co-monomer might have on overall ion transport, an ionogel was created using a covalently cross-linked poly(TFEMA) scaffold, without any MPC (*i.e* .18.7 mol% TFEMA plus 6.3 mol% PEGDA as cross-linker). This ionogel displayed an E_a value of 29.3 kJ mol^{-1} (data not shown), essentially matching that of the 1 M ILE, which suggests that the poly(TFEMA) portion of the ionogel copolymer network for samples A-G does not provide any substantial reduction to the barrier for overall ion transport in these materials.

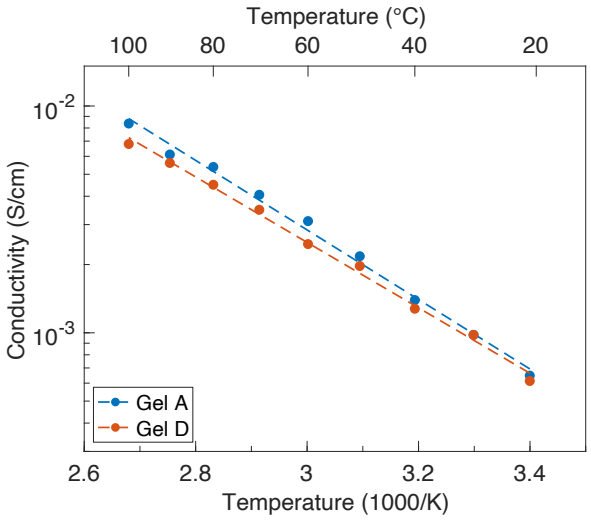

Figure 7. Temperature dependence of the ionic conductivity of ionogels A and D. Dashed lines indicate best fit regressions to an Arrhenius model, equation (2).

In order to investigate whether the poly(MPC-co-TFEMA) scaffolds examined in this study could selectively boost lithium ion transport, as had been previously observed for the poly(MPC) homopolymer,[24] lithium transference number values (t_{Li^+}) were measured for ionogels A, D, and G, and for their corresponding parent ILEs (1 M and 0.3 M Li^+). The t_{Li^+} values obtained for ionogels A and D (0.24 and 0.23, respectively) were unchanged compared to that of their parent 1 M ILE (0.23), within the margin of experimental error (± 0.1). For ionogel G, its measured t_{Li^+} value (0.20) was found to be slightly lower than that of its parent 0.3 M ILE (0.25). It is likely that the lack of any significant increase in t_{Li^+} compared to that of the parent ILE for the copolymer-supported ionogels in this study can be attributed to the ZI MPC repeat units being "diluted" by TFEMA units in the copolymer scaffold (see Fig. 2), which likely eliminates the potential for a t_{Li^+} value boost comparable to what had been observed for the ZI homopolymer in a previous study.[24] In other words, incorporating a non-ZI co-monomer (TFEMA) into the scaffold is believed to interrupt the formation of extended ZI MPC pathways, which would exist naturally for an MPC homopolymer, negating the ability to selectively boost lithium ion mobility.

Finally, because the ionogels studied in this work are enabled solely by noncovalent ZI cross-links, we preliminarily examined the feasibility of a technique to produce these ionogels "on demand" from a pre-made ZI copolymer solution. In this alternative approach, a ZI copolymer/ionic liquid solution is first prepared via UV-initiated photopolymerization in the absence of lithium salt, thus preventing the formation of any Li^+-mediated cross-links (and consequently, no gelation occurs). Next, when gel formation is desired, an appropriate quantity of Li^+-containing ILE is added and mixed into this copolymer solution, which introduces the lithium

cations necessary to form cross-links between the ZI groups and generate a freestanding ionogel. As described further in the Supporting Information, while this technique was successfully used to produce an ionogel on demand, its elastic modulus was measured to be nearly two orders of magnitude lower than that of a corresponding ionogel having the same nominal composition that was produced by the one-pot, *in situ* photopolymerization approach employed throughout the rest of this study (see Fig. S6). This finding indicates the realization of a significantly lower cross-link density within the "on demand" ionogel compared to its *in situ* analog, which may be explained by the difference in cross-link formation/self-assembly between the two approaches. As described above, it is hypothesized that doubly-coordinated MPC-Li^+-MPC complexes, which may later become cross-links between chains upon photopolymerization, are first formed within the precursor solution during the *in situ* ionogel fabrication process. In contrast, the "on demand" gelation approach begins with a solution of pre-made copolymer, which then requires the bridging of two ZI phosphorylcholine groups on neighboring polymer chains by a lithium cation from the added ILE in order for a cross-link to form. The significant reduction in ZI unit mobility as a polymer pendant group compared to the monomeric form in solution therefore likely limits the density of Li^+-mediated cross-links that can be formed via the "on demand" approach.

Conclusions

This study has examined the physical (elastic modulus, high temperature stability) and electrochemical (total ionic conductivity and its apparent activation energy, Li^+ transference number) properties of a series of ionogels synthesized by *in situ* photopolymerization of a phosphorylcholine-type ZI monomer (MPC) together with a non-ZI comonomer (TFEMA) within the ILE composed of LiTFSI dissolved in BMP TFSI. The combined amount of both monomers

in the gel precursor solution was held constant at 25 mol%, while the ZI fraction and Li^+ concentration in the ILE were both systematically varied for the first time. Control experiments confirmed that both the ZI monomer and Li^+ ions are required in order to form freestanding ionogel materials. Given the linear nature of the copolymer, the presence of robust, noncovalent interchain cross-links within these ionogels, likely in the form of Li^+-bridged ZI groups, is hypothesized. These particular noncovalent cross-links were observed to possess excellent thermal stability, resulting in no decrease in ionogel elastic modulus after being heated at 200 °C for 45 min. Experimental findings, including the variation in the minimum MPC:Li^+ molar ratio necessary to form a freestanding gel with ILE Li^+ concentration, support the notion that doubly-coordinated MPC-Li^+-MPC complexes assembled initially within the precursor solution are likely responsible for cross-link formation following photopolymerization. For the ionogel synthesized using 17.4 mol% MPC in 1 M ILE, a high elastic modulus of approximately 11 MPa was obtained. While good room temperature total ionic conductivity values (~1 mS cm^{-1}) were maintained across the various ionogel formulations examined, no improvement in the t_{Li^+} values was observed compared to those of the parent ILEs. This finding was attributed to the disruption of extended poly(ZI) pathways along the polymer scaffold by the inclusion of a non-ZI comonomer. Finally, a "gel on-demand" approach was introduced and contrasted with the *in situ* UV photopolymerization utilized in the rest of this work. The insights obtained from this study reveal important details regarding the nature of the Li^+-mediated noncovalent cross-links formed within these nonaqueous, ZI polymer-supported ionogel systems, which can aid in the design of future energy storage devices featuring safer, IL-based electrolytes.

Acknowledgements

The authors thank Dr. Ayşe Asatekin and her research group in the Tufts University Department of Chemical and Biological Engineering for generously providing the MPC and TFEMA monomers. This work was performed with support from the National Science Foundation (CBET-1802729).

Supporting Information

Example EIS and chronoamperometry data, additional gelation data, tabulated ionogel formulation and property data, sample stress vs. strain data, ionogel TGA data, and a description of the "on-demand" gelation method and results (PDF)

References

(1) Balakrishnan, P. G.; Ramesh, R.; Prem Kumar, T. Safety Mechanisms in Lithium-Ion Batteries. *J. Power Sources* **2006**, *155* (2), 401–414. https://doi.org/10.1016/j.jpowsour.2005.12.002.

(2) Xue, Z.; He, D.; Xie, X. Poly(Ethylene Oxide)-Based Electrolytes for Lithium-Ion Batteries. *J. Mater. Chem. A* **2015**, *3* (38), 19218–19253. https://doi.org/10.1039/C5TA03471J.

(3) Hu, Z.; Xian, F.; Guo, Z.; Lu, C.; Du, X.; Cheng, X.; Zhang, S.; Dong, S.; Cui, G.; Chen, L. Nonflammable Nitrile Deep Eutectic Electrolyte Enables High-Voltage Lithium Metal Batteries. *Chem. Mater.* **2020**, *32* (8), 3405–3413. https://doi.org/10.1021/acs.chemmater.9b05003.

(4) Fu, C.; Homann, G.; Grissa, R.; Rentsch, D.; Zhao, W.; Gouveia, T.; Falgayrat, A.; Lin, R.; Fantini, S.; Battaglia, C. A Polymerized-Ionic-Liquid-Based Polymer Electrolyte with High Oxidative Stability for 4 and 5 V Class Solid-State Lithium Metal Batteries. *Adv. Energy Mater.* **2022**, *12* (27), 2200412. https://doi.org/10.1002/aenm.202200412.

(5) Lewandowski, A.; Świderska-Mocek, A. Ionic Liquids as Electrolytes for Li-Ion Batteries—An Overview of Electrochemical Studies. *J. Power Sources* **2009**, *194* (2), 601–609. https://doi.org/10.1016/j.jpowsour.2009.06.089.
(6) Watanabe, M.; Thomas, M. L.; Zhang, S.; Ueno, K.; Yasuda, T.; Dokko, K. Application of Ionic Liquids to Energy Storage and Conversion Materials and Devices. *Chem. Rev.* **2017**, *117* (10), 7190–7239. https://doi.org/10.1021/acs.chemrev.6b00504.
(7) Tang, X.; Lv, S.; Jiang, K.; Zhou, G.; Liu, X. Recent Development of Ionic Liquid-Based Electrolytes in Lithium-Ion Batteries. *J. Power Sources* **2022**, *542*, 231792. https://doi.org/10.1016/j.jpowsour.2022.231792.
(8) Long, L.; Wang, S.; Xiao, M.; Meng, Y. Polymer Electrolytes for Lithium Polymer Batteries. *J. Mater. Chem. A* **2016**, *4* (26), 10038–10069. https://doi.org/10.1039/C6TA02621D.
(9) Watanabe, M.; Dokko, K.; Ueno, K.; Thomas, M. L. From Ionic Liquids to Solvate Ionic Liquids: Challenges and Opportunities for Next Generation Battery Electrolytes. *Bull. Chem. Soc. Jpn.* **2018**, *91* (11), 1660–1682. https://doi.org/10.1246/bcsj.20180216.
(10) Guo, P.; Su, A.; Wei, Y.; Liu, X.; Li, Y.; Guo, F.; Li, J.; Hu, Z.; Sun, J. Healable, Highly Conductive, Flexible, and Nonflammable Supramolecular Ionogel Electrolytes for Lithium-Ion Batteries. *ACS Appl. Mater. Interfaces* **2019**, *11* (21), 19413–19420. https://doi.org/10.1021/acsami.9b02182.
(11) Fang, Y.; Cheng, H.; He, H.; Wang, S.; Li, J.; Yue, S.; Zhang, L.; Du, Z.; Ouyang, J. Stretchable and Transparent Ionogels with High Thermoelectric Properties. *Adv. Funct. Mater.* **2020**, *30* (51), 2004699. https://doi.org/10.1002/adfm.202004699.
(12) Li, G.; Guan, X.; Wang, A.; Wang, C.; Luo, J. Cations and Anions Regulation through Zwitterionic Gel Electrolytes for Stable Lithium Metal Anodes. *Energy Storage Mater.* **2020**, *24*, 574–578. https://doi.org/10.1016/j.ensm.2019.06.030.
(13) Neitzel, A. E.; De Hoe, G. X.; Tirrell, M. V. Expanding the Structural Diversity of Polyelectrolyte Complexes and Polyzwitterions. *Curr. Opin. Solid State Mater. Sci.* **2021**, *25* (2), 100897. https://doi.org/10.1016/j.cossms.2020.100897.
(14) Taylor, M. E.; Panzer, M. J. Fully-Zwitterionic Polymer-Supported Ionogel Electrolytes Featuring a Hydrophobic Ionic Liquid. *J. Phys. Chem. B* **2018**, *122* (35), 8469–8476. https://doi.org/10.1021/acs.jpcb.8b05985.
(15) Qin, H.; Panzer, M. J. Zwitterionic Copolymer-Supported Ionogel Electrolytes Featuring a Sodium Salt/Ionic Liquid Solution. *Chem. Mater.* **2020**, *32* (18), 7951–7957. https://doi.org/10.1021/acs.chemmater.0c02820.
(16) Sun, N.; Gao, X.; Wu, A.; Lu, F.; Zheng, L. Mechanically Strong Ionogels Formed by Immobilizing Ionic Liquid in Polyzwitterion Networks. *J. Mol. Liq.* **2017**, *248*, 759–766. https://doi.org/10.1016/j.molliq.2017.10.121.
(17) Yu, Y.; Sun, N.; Wu, A.; Lu, F.; Zheng, L. Zwitterion-Containing Electrolytes with Semi–Crystalline PVDF-Co-HFP as a Matrix for Safer Lithium-Ion Batteries. *J. Mol. Liq.* **2019**, *282*, 340–346. https://doi.org/10.1016/j.molliq.2019.03.027.
(18) D'Angelo, A. J.; Panzer, M. J. Decoupling the Ionic Conductivity and Elastic Modulus of Gel Electrolytes: Fully Zwitterionic Copolymer Scaffolds in Lithium Salt/Ionic Liquid Solutions. *Adv. Energy Mater.* **2018**, *8* (26), 1801646. https://doi.org/10.1002/aenm.201801646.

(19) Peng, X.; Liu, H.; Yin, Q.; Wu, J.; Chen, P.; Zhang, G.; Liu, G.; Wu, C.; Xie, Y. A Zwitterionic Gel Electrolyte for Efficient Solid-State Supercapacitors. *Nat. Commun.* **2016**, *7* (1), 11782. https://doi.org/10.1038/ncomms11782.
(20) Haraguchi, K.; Ning, J.; Li, G. Swelling/Deswelling Behavior of Zwitterionic Nanocomposite Gels Consisting of Sulfobetaine Polymer–Clay Networks. *Eur. Polym. J.* **2015**, *68*, 630–640. https://doi.org/10.1016/j.eurpolymj.2015.03.061.
(21) Ning, J.; Kubota, K.; Li, G.; Haraguchi, K. Characteristics of Zwitterionic Sulfobetaine Acrylamide Polymer and the Hydrogels Prepared by Free-Radical Polymerization and Effects of Physical and Chemical Crosslinks on the UCST. *React. Funct. Polym.* **2013**, *73* (7), 969–978. https://doi.org/10.1016/j.reactfunctpolym.2012.11.005.
(22) Xie, F.; Gao, X.; Yu, Y.; Lu, F.; Zheng, L. Dually Cross-Linked Single Network Poly(Ionic Liquid)/Ionic Liquid Ionogels for a Flexible Strain-Humidity Bimodal Sensor. *Soft Matter* **2021**, *17* (48), 10918–10925. https://doi.org/10.1039/D1SM01453F.
(23) Bu, X.; Ge, Y.; Wang, L.; Wu, L.; Ma, X.; Lu, D. Design of Highly Stretchable Deep Eutectic Solvent-based Ionic Gel Electrolyte with High Ionic Conductivity by the Addition of Zwitterion Ion Dissociators for Flexible Supercapacitor. *Polym. Eng. Sci.* **2021**, *61* (1), 154–166. https://doi.org/10.1002/pen.25564.
(24) Taylor, M. E.; Clarkson, D.; Greenbaum, S. G.; Panzer, M. J. Examining the Impact of Polyzwitterion Chemistry on Lithium Ion Transport in Ionogel Electrolytes. *ACS Appl. Polym. Mater.* **2021**, *3* (5), 2635–2645. https://doi.org/10.1021/acsapm.1c00229.
(25) Evans, J.; Vincent, C. A.; Bruce, P. G. Electrochemical Measurement of Transference Numbers in Polymer Electrolytes. *Polymer* **1987**, *28* (13), 2324–2328. https://doi.org/10.1016/0032-3861(87)90394-6.
(26) Lind, F.; Rebollar, L.; Bengani-Lutz, P.; Asatekin, A.; Panzer, M. J. Zwitterion-Containing Ionogel Electrolytes. *Chem. Mater.* **2016**, *28* (23), 8480–8483. https://doi.org/10.1021/acs.chemmater.6b04456.
(27) Yang, F.; Liu, Y.; Liu, T.; Wang, Y.; Nai, J.; Lin, Z.; Xu, H.; Duan, D.; Yue, K.; Tao, X. Fluorinated Strategies Among All-Solid-State Lithium Metal Batteries from Microperspective. *Small Struct.* **2022**, 2200122. https://doi.org/10.1002/sstr.202200122.
(28) Wang, Y.; Chen, S.; Li, Z.; Peng, C.; Li, Y.; Feng, W. In-Situ Generation of Fluorinated Polycarbonate Copolymer Solid Electrolytes for High-Voltage Li-Metal Batteries. *Energy Storage Mater.* **2022**, *45*, 474–483. https://doi.org/10.1016/j.ensm.2021.12.004.
(29) Na, W.; Lee, A. S.; Lee, J. H.; Hong, S. M.; Kim, E.; Koo, C. M. Hybrid Ionogel Electrolytes with POSS Epoxy Networks for High Temperature Lithium Ion Capacitors. *Solid State Ion.* **2017**, *309*, 27–32. https://doi.org/10.1016/j.ssi.2017.06.017.
(30) Wongittharom, N.; Wang, C.-H.; Wang, Y.-C.; Fey, G. T.-K.; Li, H.-Y.; Wu, T.-Y.; Lee, T.-C.; Chang, J.-K. Charge-Storage Performance of Li/LiFePO4 Cells with Additive-Incorporated Ionic Liquid Electrolytes at Various Temperatures. *J. Power Sources* **2014**, *260*, 268–275. https://doi.org/10.1016/j.jpowsour.2014.02.085.
(31) Andrzejewska, E. Photoinitiated Polymerization in Ionic Liquids and Its Application: Photoinitiated Polymerization in Ionic Liquids and Its Application. *Polym. Int.* **2017**, *66* (3), 366–381. https://doi.org/10.1002/pi.5255.
(32) Borodin, O.; Self, J.; Persson, K. A.; Wang, C.; Xu, K. Uncharted Waters: Super-Concentrated Electrolytes. *Joule* **2020**, *4* (1), 69–100. https://doi.org/10.1016/j.joule.2019.12.007.

(33) Penley, D.; Vicchio, S. P.; Getman, R. B.; Gurkan, B. Energetics of Li+ Coordination with Asymmetric Anions in Ionic Liquids by Density Functional Theory. *Front. Energy Res.* **2021**, *9*, 725010. https://doi.org/10.3389/fenrg.2021.725010.
(34) Haskins, J. B.; Bennett, W. R.; Wu, J. J.; Hernández, D. M.; Borodin, O.; Monk, J. D.; Bauschlicher, C. W.; Lawson, J. W. Computational and Experimental Investigation of Li-Doped Ionic Liquid Electrolytes: [Pyr14][TFSI], [Pyr13][FSI], and [EMIM][BF_4]. *J. Phys. Chem. B* **2014**, *118* (38), 11295–11309. https://doi.org/10.1021/jp5061705.

TOC Image